Strain Relaxation and Vacancy Creation in Thin Platinum Films

W. Gruber,[1] S. Chakravarty,[1,*] C. Baehtz,[2] W. Leitenberger,[3] M. Bruns,[4,6] A. Kobler,[5,6] C. Kübel,[5,6] and H. Schmidt[1,†]

[1]*Technische Universität Clausthal, Institut für Metallurgie, Clausthal-Zellerfeld, Germany*
[2]*Helmholtz Zentrum Dresden Rossendorf, Institute of Ion Beam Physics & Materials Research, Dresden, Germany*
[3]*Universität Potsdam, Institut für Physik und Astronomie, Potsdam, Germany*
[4]*Karlsruher Institut für Technologie, Institute for Applied Materials, Eggenstein-Leopoldshafen, Germany*
[5]*Karlsruher Institut für Technologie, Institute of Nanotechnology, Eggenstein-Leopoldshafen, Germany*
[6]*Karlsruher Institut für Technologie, Karlsruher Micro Nano Facility, Eggenstein-Leopoldshafen, Germany*
(Received 29 August 2011; published 19 December 2011)

Synchrotron based combined *in situ* x-ray diffractometry and reflectometry is used to investigate the role of vacancies for the relaxation of residual stress in thin metallic Pt films. From the experimentally determined relative changes of the lattice parameter a and of the film thickness L the modification of vacancy concentration and residual strain was derived as a function of annealing time at 130 °C. The results indicate that relaxation of strain resulting from compressive stress is accompanied by the creation of vacancies at the free film surface. This proves experimentally the postulated dominant role of vacancies for stress relaxation in thin metal films close to room temperature.

DOI: 10.1103/PhysRevLett.107.265501 PACS numbers: 61.72.jd, 61.05.cf, 68.60.Bs, 81.05.Bx

Thin metal films with a thickness in the nanometer to the micrometer range are important for various areas of science and technology: microelectronics, optoelectronics, data storage, microelectromechanical systems (MEMS), catalysts, hard and abrasive coatings, and environmental and chemical protection. Devices in these fields all depend critically on the microstructure, the properties, and the stability of thin metal films deposited on appropriate substrates. Important characteristics are residual stress and strain, which often develop in film-substrate combinations [1–3]. An unfavorable consequence of high stress is crack formation, local plastic deformation, and layer delamination [4]. Consequently, understanding and controlling stress in thin films is an important task in modern technology.

Residual stresses, which are commonly assumed to be biaxial in thin films, result from different thermal expansion coefficients of substrate and film (thermal stress) and/or from stress formation during film deposition (grown-in stress). During isothermal annealing residual stresses relax as a function of annealing time and temperature. This relaxation was extensively investigated in numerous studies [5–10]. Various possible microscopic mechanisms of stress relaxation were suggested, for example, diffusional creep, power law creep, grain boundary gliding, twin formation, or grain rotation [8,10–12]. In polycrystalline films close to room temperature a central mechanism that governs stress relaxation by inelastic deformation is thought to be atomic diffusion, predominantly along grain boundaries [2,3,13–15]. This is especially true for nanometer grained structures that are typical for such materials. In unpassivated metal films stresses relax almost completely above the temperature at which grain boundary diffusion can occur [14], which emphasizes the importance of this mechanism. It is suggested that stress relaxation is taking place by the transport of atoms and of the corresponding point defects between the free surface of the film and the grain boundaries due to a stress induced difference in the chemical potential [3,14]. Assuming a vacancy mechanism that commonly governs diffusion in metals [16], a flux of vacancies counterbalances the flux of atoms in the opposite direction. In the case of tensile stress, vacancies have to be transported to the surface where they are annihilated and in the case of compressive stresses vacancies have to be created at the free surface and have to migrate to the grain boundary in order to enable stress relaxation.

However, up to now no clear experimental proof was presented for a direct correlation between stress relaxation and vacancy formation or annihilation, e.g., at the free surface, which is a prerequisite for a diffusion controlled mechanism. In order to get more insight into this topic, a quantitative, quasisimultaneous *in situ* characterization of the modification of vacancy concentration and of residual strain in metallic films is necessary. In the present study we applied a method which is based on the fundamental concept of dilatometry [17,18] and which is used to study vacancies in thermal equilibrium [19]. We modified this basic concept by using an experimental arrangement that is completely based on x-ray scattering techniques. This has the advantage that the use of synchrotron radiation becomes possible, which allows us to carry out time-resolved studies to measure fast relaxation processes taking place on a time scale of minutes. In order to detect directly the modification of the vacancy concentration, x-ray diffractometry (XRD) is used to determine the of the out-of-plane lattice parameter a and x-ray reflectivity (XRR) is used to detect the film thickness (macroscopic lengths change) L. The relative change in vacancy concentration (atomic fraction) Δc for a cubic metal is then given by [19]

 © 2011 American Physical Society

$$\Delta c = \left(\frac{\Delta L}{L} - \frac{\Delta a}{a}\right), \tag{1}$$

where ΔL and Δa are the respective changes of a and L. Note that in Eq. (1) a factor of 3 is lacking in comparison to the classical formula used for bulk materials [19]. This is due to the fact that for thin films a modification of the vacancy concentration is mainly taking place at the free film surface parallel to the substrate. The time dependent relative change of the out-of-plain strain $\Delta\varepsilon$ is then given by

$$\Delta\varepsilon \approx \frac{\Delta a}{a} = \frac{1-\upsilon}{E}\Delta\sigma \tag{2}$$

assuming a biaxial stress model, where $\Delta\sigma$ is the modification of the in-plane stress during annealing, E is the bulk modulus, and ν the Poisson number.

For the experiments, about 40 nm thin Pt films were used as a model system because this element is relatively inert against oxidation. The films were deposited by magnetron sputtering on Si wafers which were thermally preoxidized (400 nm SiO_2) in order to prevent reactive diffusion. Sputtering was carried out in an argon atmosphere at a power of 200 W and a base pressure better than 10^{-6} mbar. For the *in situ* experiments XRR and XRD in symmetric $\theta/2\theta$ geometry were done at the Rossendorf beam line (ROBL) of the European Synchrotron Facility (ESRF). These experiments were performed at a wavelength of 1.08 Å ($E = 11.5$ keV) using parallel beam mode. *In situ* annealing was carried out at a temperature of 130 °C in a resistance furnace with a Be dome evacuated to 3×10^{-6} mbar which was mounted on a goniometer. The x-ray investigations were accompanied by *ex situ* transmission electron microscopy (TEM) with an imaging corrected FEI Titan 80–300 operated at 300 kV. TEM cross-section sample preparation was done by *in situ* liftout using a FEI Strata 400 S Dual-Beam focused ion beam (FIB) with the final polishing performed at 5 kV. High resolution photoelectron spectroscopy measurements using a monochromatic Al $K\alpha$ source (K-Alpha, Thermo Scientific) excluded oxide formation at the surface in the as-deposited state and after annealing of the Pt film.

Figure 1 shows cross-sectional transmission electron microscopy (TEM) bright field and dark field micrographs of an as-deposited Pt film and after *in situ* annealing at 130 °C for 15 h. From these images we see that the as-deposited sample is composed of columnar grains oriented perpendicular to the film surface. The columnar grains have diameters of about 10–20 nm and a length which is approximately the film thickness of 40 nm. The grains show a preferred (111) orientation. For the sample annealed at 130 °C, the microstructure and grain size is not significantly modified. From plain view bright field and dark field as well as HR-TEM images (not shown) a grain diameter of 10–20 nm is confirmed.

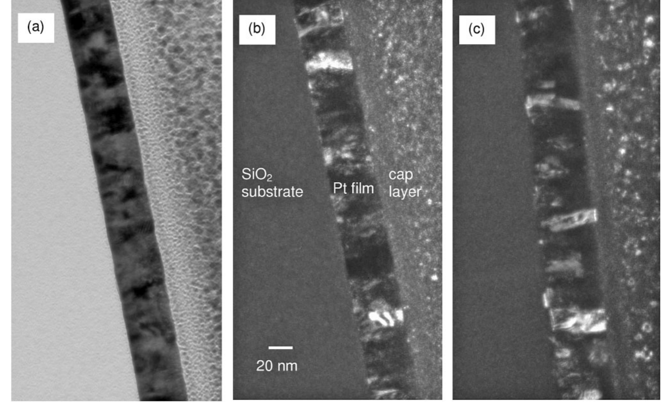

FIG. 1. Cross-sectional TEM images of (a) an as-deposited Pt film (bright field), (b) an as-deposited Pt film (dark field), and (c) a film annealed at 130 °C for 15 h (dark field). The cap layer is due to FIB preparation.

Figure 2 shows the Pt (111) Bragg peak measured by XRD for a sample annealed at 130 °C for 15 h and for the same sample cooled to room temperature afterwards. The peak position of the heated sample is located at smaller 2Θ values indicating an increase of the interplanar distance d_{111} due to thermal expansion. Bragg peaks were fitted with Lorentzians to extract exact Peak positions. The error limit of the peak position is about 3×10^{-4} deg which leads to an error of 5×10^{-5} Å in d_{111} according to the error propagation law.

Figure 3(a) shows the XRR curve of an as-deposited sample. The fringes result from the interference of the x rays reflected at the surface and at the Pt/SiO_2 interface, respectively. The thickness of the Pt film was determined using the angle (or q_z) positions of the fringe maxima as described in Ref. [20]. In addition, the whole experimentally determined XRR profile was least-squares fitted using the Parratt formalism [21] (program package PARRATT32). As is obvious from Fig. 3(a), a very good agreement is

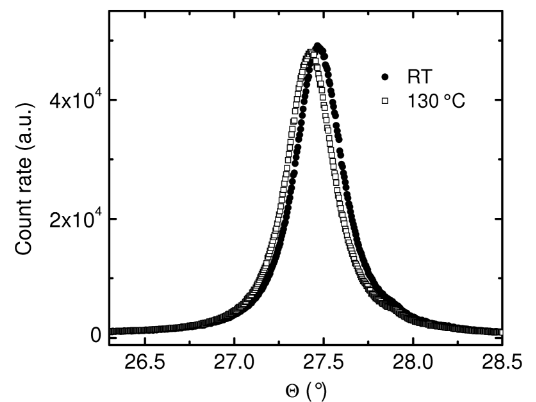

FIG. 2. (111) Bragg peak of a sample annealed at 130 °C for 15 h and of the same sample cooled down to room temperature afterwards. Shown are data where the intensity is normalized to the incoming beam.

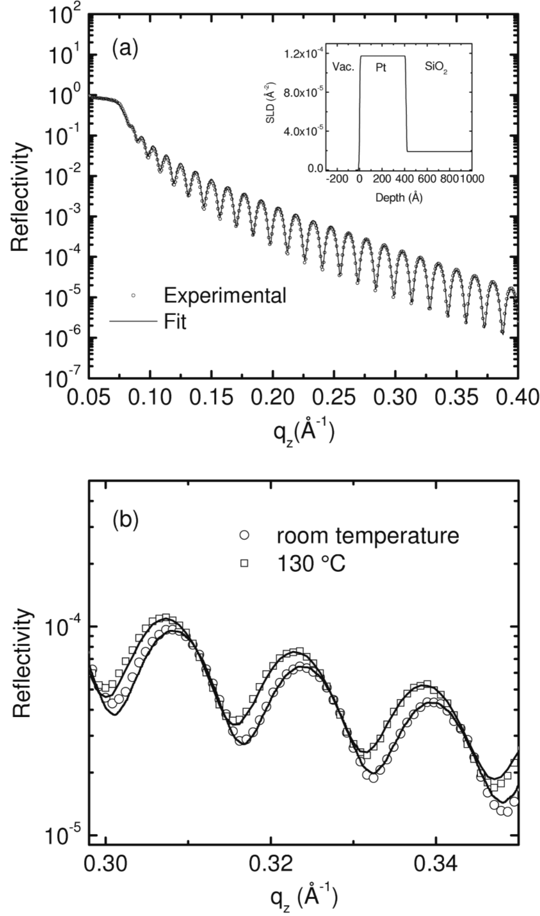

FIG. 3. (a) Experimentally determined XRR curve of an as-deposited sample. A least-squares fit using the program PARRATT32 is also shown (Pt layer thickness $L = 413.8$ Å, $\sigma(\mathrm{SiO_2/Pt}) = 4.4$ Å, $\sigma(\mathrm{Pt/vacuum}) = 4.2$ Å). The inset shows the scattering length density as obtained by the fit. (b) Zoom of XRR curves of another as-deposited sample [$L = 388.8$ Å, $\sigma(\mathrm{SiO_2/Pt}) = 4.0$ Å, $\sigma(\mathrm{Pt/vacuum}) = 5.9$ Å] and the same sample annealed at 130 °C for 15 h [$L = 389.9$ Å, $\sigma(\mathrm{SiO_2/Pt}) = 3.8$ Å, $\sigma(\mathrm{Pt/vacuum}) = 5.9$ Å].

given. The corresponding scattering length density as obtained from the fit is shown in the inset of Fig. 3(a). Surface and interface roughness is about 4 Å. In Fig. 3(b) a zoom of XRR curves for another as-deposited sample and the same sample annealed at 130 °C for 15 h is given together with Parratt fits. The clearly resolved shift in the position of the fringes corresponds to a change in the average thickness of about 1 Å. The error limit of the calculated thickness is 0.05–0.1 Å according to the error propagation law. The Parratt simulations gave the same values for the Pt layer thickness within error limits. In order to estimate the significance of the error attributed to the thickness we annealed a sample at 270 °C until L shows no further time dependence (see below). Then we measured the reflectivity several times. The standard deviation of the thicknesses derived from these measurements was 0.15 Å, which means that the errors mentioned above are reasonable. The fact that the overall intensity of the reflectivity of the annealed sample in Fig. 3(b) is slightly higher, can be explained by a tiny decrease of the surface roughness (see figure caption). This in no way influences our analysis. The roughness of the $\mathrm{Pt/SiO_2}$ interface remains constant during annealing.

The thermal expansion coefficient of Pt (9×10^{-6} K^{-1} [22]) is larger than the thermal expansion coefficient of $\mathrm{SiO_2}$ (0.6×10^{-6} K^{-1} [22]). Therefore, heating from room temperature to 130 °C leads to the formation of compressive stress parallel to the sample surface and, consequently, to an expansion of the lattice constant perpendicular to the sample surface. This thermal stress is superimposed on the already present grown-in stress. The formation of anisotropic thermal strain together with the isotropic thermal expansion is termed thermoelastic expansion of the film. At the temperature under investigation this thermoelastic expansion is reversible and it is assumed that stress relaxation is dominated by the relaxation of grown-in stress.

In order to apply Eq. (1), the relative changes in $L(T, t)$ and a (T, t) during *in situ* annealing were determined, using $\Delta L/L = [L(130, t) - L(130, 0)]/L(130, 0)$ and $\Delta a/a = [d_{111}(130, t) - d_{111}(130, 0)]/d_{111}(130, 0)$ (out-of-plane). In this expression $L(130, 0)$ and $d_{111}(130, 0)$ are the thickness and the interplanar distance after heating up to 130 °C, but before relaxation starts. These quantities cannot be measured directly, because during the heat-up procedure relaxation of L and d_{111} already takes place. In order to obtain the relative changes in L and d_{111} as shown in Figs. 4(a) and 4(b), we calculated $L(130, 0)$ and $d_{111}(130, 0)$ in the following way: after isothermal annealing for 15 h at 130 °C, relaxation is completed and the quantities $L^{\mathrm{relax}}(130)$ and $d_{111}^{\mathrm{relax}}(130)$ are measured. After cooling to room temperature both quantities were measured again and we obtain $L^{\mathrm{relax}}(\mathrm{RT})$ and $d_{111}^{\mathrm{relax}}(\mathrm{RT})$. The difference $\Delta L^{\mathrm{relax}} = L^{\mathrm{relax}}(130) - L^{\mathrm{relax}}(\mathrm{RT})$ and the corresponding value of $\Delta d_{111}^{\mathrm{relax}}$ are to a good approximation the thermoelastic changes. We added these values to the initial values measured at room temperature before annealing started in order to obtain $L(130, 0) \approx L(\mathrm{RT}, 0) + \Delta L^{\mathrm{relax}}$ and $d_{111}(130, 0) = d_{111}(\mathrm{RT}, 0) + \Delta d_{111}^{\mathrm{relax}}$. The change in vacancy concentration (atomic fraction), $\Delta c(T, t)$, can be calculated according to Eq. (1). XRR and XRD were measured consecutively. As the annealing time t we used the beginning of the XRD measurement which was performed after XRR. The result is shown in Fig. 4. We observe a clear increase of the vacancy concentration as a function of annealing time [Fig. 4(c)], while at the same time the strain is decreasing [Fig. 4(a)].

The results shown in Figs. 4(a) and 4(c) can be explained with the following model. For the present nanostructural arrangement all the grain boundaries are expected to be under an identical normal stress. During isothermal annealing vacancies are created at the free surface of the Pt film.

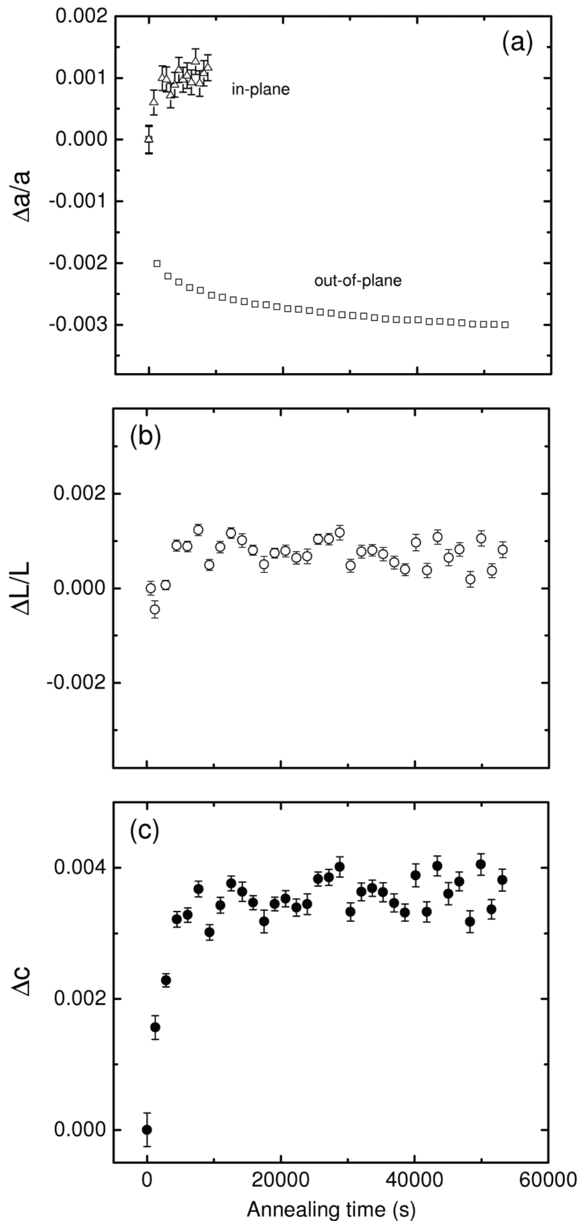

FIG. 4. Relative changes (a) of the out-of-plane lattice parameter a and of the in-plane lattice parameter (b) of the thickness L and (c) of the vacancy concentration (atomic fraction) Δc as a function of annealing time at 130 °C. Where no error limits are indicated, they are less than the diameter of the symbol.

This is reflected in the observed increase of Δc in Fig. 4(c). Since these vacancies are assumed to be highly mobile (activation energy: about 0.5–0.8 eV) [23] at the surface they diffuse to the grain boundaries and penetrate the film along the grain boundaries. Volume diffusion is expected to be frozen in at the temperature under investigation (activation energy: 2.7 eV) [16]. At the grain boundaries a process has to take place which results in a reduction of the biaxial stress. This relaxation process may take place by a gap closure process as illustrated in Ref. [13]. The arrival of the vacancies at the grain boundary creates an extra free volume or a "gap" at the grain boundary. To maintain the low equilibrium vacancy concentration in the grain boundary, the crystal will tend to annihilate these vacancies immediately, eliminating the free volume by closing the grain boundary gap. Such a gap closure process results in lateral film shrinkage and consequently in a reduction of compressive stress in the direction parallel to the film surface and also of the out-of-plane lattice parameter as shown in Fig. 4(a). The in-plane lattice parameter was also measured in a different experimental session using energy-dispersive XRD and a similar setup. As is obvious from Fig. 4(a), we found a continuous increase of the in-plane lattice parameter during annealing in accordance with the suggested model. However, since the data were not obtained during the same experiment, they are not used for a further quantitative analysis.

Please also note that the increase in vacancy concentration of almost half of a per cent as shown in Fig. 4(c) cannot be associated with the equilibrium value in the film, which is expected to be much lower. What is measured here is the creation of vacancies at the free surface. Afterwards these vacancies diffuse to the grain boundary, are annihilated, and further vacancies are created in order to enable a continuous stress relaxation.

It has to be noted that vacancy creation as the dominating process cannot be unambiguously identified from Fig. 4(c). In principle, all other types of volume-assisted defects like multiple vacancies, nanovoids, or interstitials may lead to the same behavior. A significant role of interstitials in the observed process is, however, very unlikely, because interstitial annihilation [which could also explain the results in Fig. 4(c)] is taking place in Pt at and below room temperature [24]. A significant amount of nanoscopic voids was not detected by TEM imaging. However, the presence of multiple vacancies or small vacancy clusters cannot be completely ruled out at the present stage of the study. Nevertheless, the explanation of our results based on vacancy creation is the most likely explanation. In addition, the free surface of the film might not be the only source of vacancies. At present we cannot exclude the existence of a low density layer between Pt and SiO_2 (see, e.g., Ref. [25]), which might also be a source of vacancies. However, such a layer is not supported by the PARRATT32 simulations of Fig. 3(b).

In conclusion, our experiments suggest that strain relaxation in thin Pt films close to room temperature is correlated to the generation of vacancies at the free surface of the film. These vacancies are expected to diffuse to the grain boundaries, where stress can be released. The measurements prove the dominant role of vacancies for stress relaxation in thin metal films at low temperatures and support a diffusion controlled relaxation mechanism.

We acknowledge the European Synchrotron Radiation Facility for provision of synchrotron radiation facilities and we would like to thank the staff for assistance in using

beamline BM20. We further thank the Helmholtz-Zentrum Berlin-BESSY II for the realization of the in-plane lattice parameter measurement. This work was partially carried out with the support of the Karlsruhe Nano Micro Facility (KNMF), a Helmholtz Research Infrastructure at Karlsruhe Institute of Technology. We thank M. Horisberger (Paul-Scherrer-Institute, Switzerland) for the deposition of the Pt films. This research has been supported by the German Research Foundation under Contract No. Schm1569/13-1.

*Present address: UGC-DAE Consortium for Scientific Research, Kalpakkam 603102, India.
†Corresponding author.

[1] G. C. A. M. Janssen, Thin Solid Films **515**, 6654 (2007).
[2] M. F. Doerner and W. D. Nix, Crit. Rev. Solid State Mater. Sci. **14**, 225 (1988).
[3] M. D. Thouless, Annu. Rev. Mater. Sci. **25**, 69 (1995).
[4] A. G. Evans, M. D. Drory, and M. S. Hu, J. Mater. Res. **3**, 1043 (1988).
[5] S. Hyun, W. L. Brown, and R. P. Vinci, Appl. Phys. Lett. **83**, 4411 (2003).
[6] Soo-Jung Hwang, Yong-Duck Lee, Young-Bae Park, Je-Hun Lee, Chang-Oh Jeong, and Young-Chang Joo, Scr. Mater. **54**, 1841 (2006).
[7] D. W. Gan, P. S. Ho, R. Huang, J. Leu, J. Maiz, and T. Scherban, J. Appl. Phys. **97**, 103531 (2005).
[8] W. Brückner and V. Weihnacht, J. Appl. Phys. **85**, 3602 (1999).
[9] M. Hershkovitz, I. A. Blech, and Y. Komem, Thin Solid Films **130**, 87 (1985).
[10] M. Murakami, Thin Solid Films **55**, 101 (1978).
[11] A. Gangulee, Acta Metall. **22**, 177 (1974).
[12] L. I. Trusov, T. P. Khvostantseva, and V. A. Melnikova, J. Mater. Sci. **30**, 2956 (1995).
[13] S. Nakahara, S. Ahmed, T. T. Ahmed, and D. N. Buckley, J. Electrochem. Soc. **154**, D145 (2007).
[14] H. Gao, L. Zhang, D. Nix, C. V. Thompson, and E. Arzt, Acta Mater. **47**, 2865 (1999).
[15] D. Weiss, H. Gao, and E. Arzt, Acta Mater. **49**, 2395 (2001).
[16] H. Mehrer, *Diffusion in Solids* (Springer, New York, 2007).
[17] H.-E. Schaefer, K. Frenner, and R. Wurschum, Phys. Rev. Lett. **82**, 948 (1999).
[18] B. Oberdorfer, B. Lorenzoni, K. Unger, W. Sprengel, M. Zehetbauer, R. Pippan, and R. Wurschum, Scr. Mater. **63**, 452 (2010).
[19] Y. Kraftmakher, Phys. Rep. **299**, 79 (1998).
[20] V. Holý, U. Pietsch, and T. Baumbach, *High-Resolution X-Ray Scattering from Thin Films and Multilayers* (Springer, New York, 1999), p. 120.
[21] L. G. Parratt, Phys. Rev. **95**, 359 (1954).
[22] D. R. Lide, *CRC Handbook of Chemistry and Physics* (CRC Press, Boca Raton, 2010).
[23] D. W. Basset and D. R. Webber, Surf. Sci. **70**, 520 (1978).
[24] W. Schüle, Z. Metallkd. **89**, 11 (1998).
[25] X. L. Li, B. Chen, H. Y. Jing, H. B. Lu, B. R. Zhao, Z. H. Mai, and Q. J. Jia, Appl. Phys. Lett. **87**, 222905 (2005).